Observation of magnetization saturation in the S=1 one-dimensional Heisenberg antiferromagnets $Ni(C_2H_8N_2)_2NO_2(ClO_4)$ and $CsNiCl_3$

1995 J. Phys.: Condens. Matter 7 5881

(http://iopscience.iop.org/0953-8984/7/29/015)

J. Phys.: Condens. Matter 7 (1995) 5881–5890. Printed in the UK

Observation of magnetization saturation in the $S = 1$ one-dimensional Heisenberg antiferromagnets $Ni(C_2H_8N_2)_2NO_2(ClO_4)$ and $CsNiCl_3$

H Nojiri†, Y Shimamoto†, N Miura† and Y Ajiro‡

† Institute for Solid State Physics, University of Tokyo, 7-22-1 Roppongi, Tokyo 106, Japan

‡ Department of Applied Physics, Fukui University, Bunkyo, Fukui 910, Japan

Received 6 March 1995

Abstract. The magnetization in $S = 1$ one-dimensional Heisenberg antiferromagnets $Ni(C_2H_8N_2)_2NO_2(ClO_4)$ (NENP) and $CsNiCl_3$ was measured by means of the Faraday rotation in ultrahigh magnetic fields up to 150 T. A distinct saturation of the magnetization was observed in both samples. From the saturation field, the exchange coupling constants are evaluated as $J = 45.5$ K and 25.8 K for NENP and $CsNiCl_3$, respectively. The experimental magnetization curve is in good agreement with a theoretical curve for an $S = 1$ one-dimensional Heisenberg antiferromagnet at finite temperatures.

1. Introduction

Low-dimensional quantum spin systems have attracted much attention in these decades both theoretically and experimentally. One of the most interesting theoretical studies on these quantum spin systems is by Haldane [1]. Haldane predicted that there is an energy gap between the non-magnetic singlet ground state and the lowest excited triplet state in a one-dimensional Heisenberg antiferromagnet with integer spins. Since this prediction was reported, many experimental studies have been performed on $S = 1$ Heisenberg antiferromagnets which contain Ni^{2+} ions.

Buyers *et al* [2] and subsequently Steiner *et al* [3] performed the first experimental studies to confirm Haldane's prediction on $CsNiCl_3$ by means of inelastic neutron scattering. For more than two decades, intensive investigations have been made on the magnetism in $CsNiCl_3$ from the viewpoint of low-dimensional magnetism, especially as a model material of triangular antiferromagnets. Achiwa [4] found that the magnetic susceptibility of $CsNiCl_3$ shows a typical temperature dependence of one-dimensional Heisenberg antiferromagnets with a peak of around 35 K [4]. Achiwa also observed three-dimensional magnetic ordering below 4.5 K. The magnetic structure of this ordered phase was determined by neutron scattering experiments [5–7]. These experiments show that magnetic moments form antiferromagnetic chains along the c axis and weak interchain coupling causes the triangular structure in the c plane. Clark and Moulton [8] found evidence of successive phase transitions at $T_{N1} = 4.84$ K and $T_{N2} = 4.40$ K by NMR. The existence of the successive transitions was also confirmed by measurements of the heat capacity [9]. According to a neutron diffraction experiment, only the c-axis component of the magnetic moment is ordered at temperatures between T_{N1} and T_{N2} [10]. The fundamental parameters of $CsNiCl_3$ such as an intrachain or interchain coupling constant and anisotropy are summarized in [11, 12]. The ratio of the interchain coupling J' to the interchain coupling J is the range

0953-8984/95/295881+10$19.50

$J'/J = (0.2\text{–}5) \times 10^{-2}$. It has a relatively small Ising-type anisotropy D along the c axis. The reported value of D is in the range $D/J = (0.2\text{–}0.6) \times 10^{-2}$. These small values of the parameters show that $CsNiCl_3$ has the properties of an $S = 1$ one-dimensional Heisenberg antiferromagent. However, it is not an ideal model material to test Haldane's prediction, because it shows three-dimensional long-range order below T_N. The existence of the magnetic ordering makes it difficult to examine the nature of the non-magnetic ground state which appears below the temperature corresponding to the Haldane gap energy.

Besides $CsNiCl_3$, Renard *et al* [13] proposed that $Ni(C_2H_8N_2)_2NO_2(ClO_4)$ (NENP) could be a model material of the Haldane system. Meyer *et al* [14] examined the crystal structure of NENP and found that it consists of $Ni(C_2H_8N_2)_2NO_2$ chains along the b axis. The exchange coupling along the chain was evaluated by their susceptibility measurement as $J = 47.5$ K. Renard *et al* performed experiments on susceptibility measurement and inelastic neutron scattering. An abrupt decrease in the susceptibility was found below 15 K and no long-range order was observed at low temperatures down to 1.2 K. From the magnetic dispersion, they found two energy gaps $E_{g\parallel} = 30$ K and $E_{g\perp} = 14$ K, for parallel and perpendicular directions, respectively, to the b axis. The ratio of the interchain coupling J' to the intrachain coupling J was estimated to be $J'/J = 4 \times 10^{-4}$ by their experiment on the magnetic dispersion. The small value of J'/J proved the one-dimensional character of NENP.

Since its discovery, many experimental results have been reported on NENP. Ajiro *et al* [15] and Katsumata *et al* [16] measured the magnetization curve of NENP up to 40 T and 50 T, respectively. They found an abrupt increase in the magnetization at around a critical field $H_c = 7.5\text{–}13.1$ T depending on the sample orientations. This anomaly is considered to be due to a transition from the non-magnetic ground state to an excited state which occurs under the condition when the Zeeman energy exceeds the Haldane gap energy. Parkinson and Bonner [17] calculated magnetization of finite-size systems at $T = 0$ K by numerical diagonalizations. Sakai and Takahashi [18] obtained a full magnetization curve at $T = 0$ K in the thermodynamic limit by applying a finite-size scaling based on the conformal field theory to numerical diagonalizations. Recently, Yamamoto and Miyashita [19] performed a quantum Monte Carlo simulation in both periodic and open boundary conditions and calculated the magnetization curve at finite temperatures.

It is interesting to measure the magnetization curve up to saturation and to compare the results with these theories to study the behaviour of Haldane gap materials in magnetic fields. It is also useful to measure the saturation field because the exchange coupling constant J can be evaluated directly from the saturation field.

A special technique is required to observe the saturation of the magnetization in NENP and $CsNiCl_3$ because the saturation field exceeds the range which can be reached by non-destructive pulsed magnets. In the case of an $S = 1$ one-dimensional Heisenberg antiferromagnet with $g = 2$, the saturation field of 100 T corresponds to the exchange constant of $J = 33.6$ K, which is comparable with the exchange constant reported for $CsNiCl_3$. In the case of NENP, the reported value of J is roughly 1.5 times larger than that of $CsNiCl_3$ and therefore the saturation field is expected to be higher than 100 T. In the present work, we performed Faraday rotation measurements up to 150 T by using the single-turn coil technique. In the following, the result of the Faraday rotation experiments and the comparison between the experimental and theoretical magnetization curves is discussed.

2. Experimental details

In magnetic fields higher than 100 T (megagauss fields), ordinary magnetization

measurement by using the inductive pick-up coil method is an extremely difficult task. It is because of a large induction voltage which is proportional to the time derivative of the magnetic flux. The typical rise time of the megagauss field is much shorter than that for non-destructive pulsed fields. It is about a few microseconds and hence the induction voltage is about 1000 times larger than that of the non-destructive pulsed fields. Therefore, in the present work, we performed measurements of Faraday rotation instead of the ordinary magnetization measurements because such an optical method is not affected by the large induction voltages.

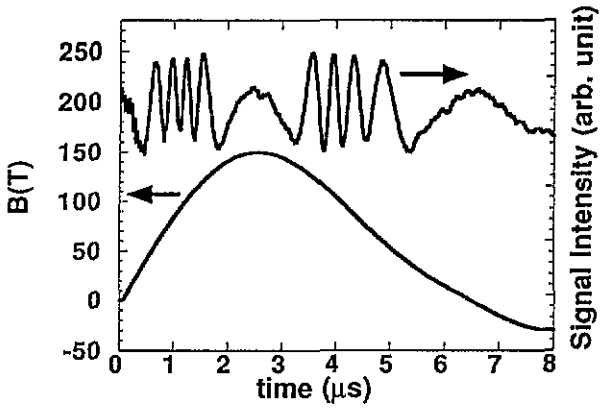

Figure 1. Trace of the magnetic field and an example of Faraday rotation data at a wavelength of 1152 nm for NENP. The thickness of the sample is 0.8 mm.

The single-turn coil technique is used to generate magnetic fields higher than 100 T [20]. Figure 1 shows a trace of a magnetic field produced by this technique and an example of the Faraday rotation data. Magnetic fields up to 150 T are available with a bore of 10 mm. The shape of the pulsed field is sinusoidal with a half-period of about 6 μs. After every shot, the coil is destroyed for the strong electromagnetic force; however, it almost keeps the original form in a period of several microseconds for inertia. In spite of the complete destruction of the coil, the sample set at the centre of the coil remains unbroken because the coil blows up towards the outer direction.

The Faraday rotation angle is composed of both magnetic and non-magentic parts. As is well known, the magnetic part of the Faraday rotation is expressed in the odd-power series of the magnetization. That is, the rotation angle θ is expressed as follows:

$$\theta = \theta_0(H) + A_1 M + A_3 M^3 + A_5 M^5 + \cdots \tag{1}$$

where $\theta_0(H)$ is a non-magnetic part, M is the magnetization and $A_1, A_3, \ldots$, are coefficients. In practice, the non-magentic contribution $\theta_0(H)$ for NENP and $CsNiCl_3$ is very small and it can be neglected, as will be discussed in the next section. In low magnetic fields, the rotation angle is almost linear with respect to the magnetization. In the higher-field range, contributions of higher-order terms in equation (1) should be considered. The microscopic origin of the magnetic Faraday rotation is the spin–orbit splitting in the excited states. It causes a difference between the transition probabilities of the right and left circularly polarized lights in the transition from the ground Γ_2 orbit to excited Γ_5 or Γ_4 orbits in the ^3F state of Ni^{2+}. When the photon energy of the incident light is close to the transition energy between the Γ_2 orbit and excited orbits, the contribution of the higher-order terms in the Faraday rotation should be taken into account and the rotation angle becomes non-linear

to the magnetization. This non-linearity is negligibly small when the photon energy of the incident light is considerably lower than this transition energy.

The energy level splitting for $CsNiCl_3$ was measured by Ackerman *et al* [21]. According to their results, the Γ_2–Γ_5 energy splitting is 6855 cm^{-1} (0.85 eV) and the Γ_2–Γ_4 splitting is 11 315 cm^{-1} (1.4 eV). There is no information about the value of these energy levels so far reported for NENP. In the present work, we used two different laser lines at 632.8 nm (1.96 eV) and 1152 nm (1.08 eV). These energies are comparable with the energy splitting of the ^3F state. As a consequence, a large contribution of the higher-order terms was observed in the present experiments. We corrected the higher-order terms in equation (1) by comparing the Faraday rotation with the magnetization data obtained by non-destructive pulsed magnets.

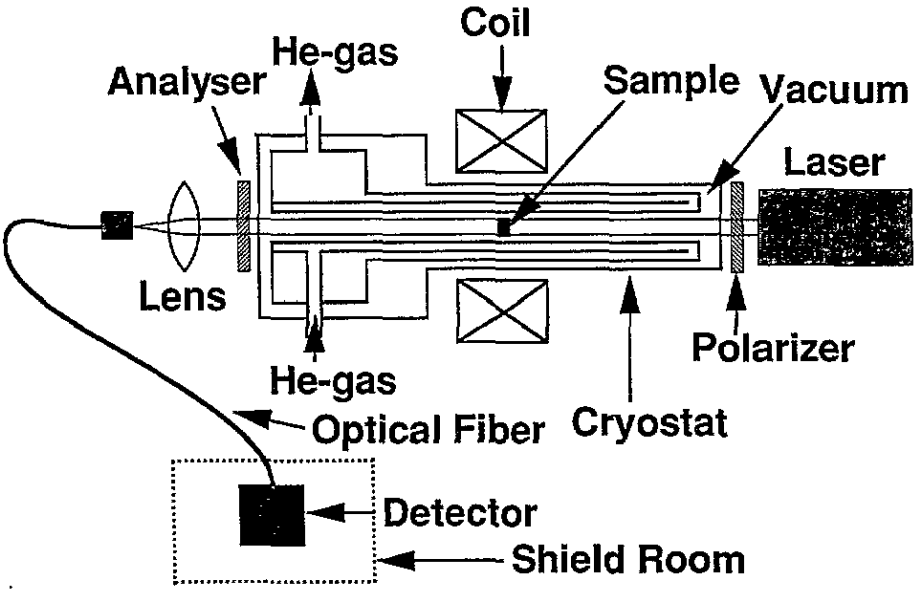

Figure 2. Schematic diagram of the experimental set-up for Faraday rotation measurement. A cryostat is made from plastic to avoid the destruction of the cryostat by the strong electromagnetic forces in megagauss fields.

Figure 2 shows the experimental set-up for the Faraday rotation experiment. The light from the red He–Ne laser (632.8 nm) or the near-infrared He–Ne laser (1152 nm) is first linearly polarized with a polarizer. The sample is located in a gas-flow-type cryostat made from plastic. A temperature as low as 10 K is available with this cryostat. The polarization of the transmitted light is analysed with an analyser which is set in the back of the sample. A lens system and an optical fibre were used for the light guide. The intensity of the light led into a shield room is measured with a detector. The use of an optical fibre is essential to decrease the effect of the discharge noise of large current as high as 2 MA in the single-turn coil system. An avalanche photodiode or a Si–p–i–n photodiode is used as a detector. The cut-off frequency of these detectors was 60–100 MHz which is sufficiently high for the short pulse period of a few microseconds. The magnetic field intensity was measured using a pick-up coil. The error in the magnetic field intensity was less than 1%. The optical and magnetic field signals were digitized and stored by transient recorders and then analysed by

a computer. From the trace of the Faraday rotation signal as shown in figure 1, the rotation angle was obtained by an arcsine transformation.

Single-crystal samples of NENP and $CsNiCl_3$ were used for the measurement. These were cut along their cleaved planes. In the case of NENP, the cleavage plane is perpendicular to the *a* axis and the magnetic field was applied along this axis. The direction of injected light is perpendicular to the (1120) or (1210) face in the case of the $CsNiCl_3$.

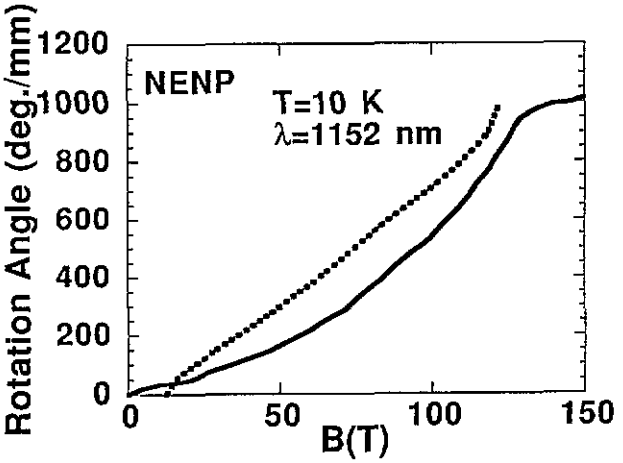

Figure 3. Plot of the rotation angle for NENP against the magnetic field: ·····, magnetization curve at $T = 0$ K calculated by Sakai and Takahashi [18].

3. Results

Figure 3 shows a plot of the Faraday rotation angle versus the magnetic field at 10 K at a wavelength of 1152 nm (1.08 eV) for NENP. It shows a distinct saturation at around 130 T. The rotation angle at 150 T is about 1000° mm^{-1}. The small zigzag on the experimental curve is caused by the error in the arcsine transformation from the raw data to derive the rotation angle. This is because the resolution in converting the signal to the rotation angle is poor around the peak and bottom of the sinusoidal function. The Faraday rotation data have a large deviation from the theoretical magnetization curve obtained by Sakai and Takahashi [18] for $T = 0$ K as shown in figure 3. The deviation around the saturation field H_s is due to the effect of the finite temperature which causes rounding of the magnetization curve. The Faraday rotation data in the intermediate field between the critical field H_c and H_s show a large deviation from the theoretical curve, which has an almost linear slope to the magnetic field. This deviation is caused by the contribution of the higher-order terms of the magnetic Faraday rotation as shown in equation (1). Since no spectroscopy data have been reported so far in the near-infrared and visible ranges for NENP, there are no reliable values for the energy splitting of the Γ_2–Γ_5 and Γ_2–Γ_4 transitions. Considering the facts that the transmission is very low at both 632.8 nm and 1152 nm and that the colour of the sample is dark red, we can postulate that there are absorption bands in the red and near-infrared ranges in a similar way to the case of $CsNiCl_3$.

The Faraday rotation angle in $CsNiCl_3$ is plotted as a function of magnetic field in figure 4. The wavelength is 632.8 nm (1.96 eV). The transmission at 1152 nm (1.08 eV) was so low that the measurements were performed only at 632.8 nm. The strong absorption

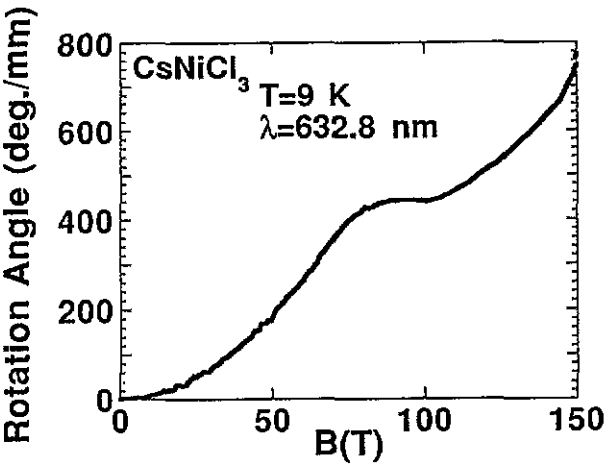

Figure 4. Plot of the rotation angle for $CsNiCl_3$ against the magnetic field. There is a plateau in the range 75–100 T showing saturation of the magnetization. The Faraday rotation shows an increase above 110 T as discussed in section 4.

at 1152 nm may be related to the Γ_2–Γ_5 transition energy which was determined to be 6855 cm^{-1} (0.85 eV) by Ackerman *et al* [21]. The Faraday rotation angle in figure 4 shows a large deviation from the theoretical magnetization curve by Sakai and Takahashi at $T = 0$ K, as is plotted in figure 3. Saturation of the Faraday rotation is observed at around 75 T. However, the rotation angle shows a subsequent increase again above 110 T. The Faraday rotation angle is 450° mm^{-1} at 100 T. The saturation field of 75 T is consistent with the reported exchange constant [4, 11, 12]. We thus considered that the saturation at 75 T is related to the magnetization saturation. The reason for the increase in the Faraday rotation angle above 110 T is not clear at present. In the magnetization process up to 75 T, the contribution of the higher-order terms is important, in a similar fashion to the result for NENP. The large contribution of the higher-order terms can be explained considering the fact that the splitting of Γ_2–Γ_4 as 11315 cm^{-1} (1.4 eV) is close to the photon energy at 632.8 nm. The effect of the finite temperature is also found in the rounding of the kink in the rotation angle versus field curve at the saturation $H_s \sim 75$ T. It is very pronounced compared with the result for NENP. In the case of $CsNiCl_3$, the exchange constant is about two thirds of that of NENP. Therefore, we expect a larger effect of the thermal fluctuation at the same temperature.

4. Discussion

First, we discuss the contribution of the non-magnetic part and the higher-order terms in magnetic Faraday rotation to convert the Faraday rotation data to the magnetization. Figure 3 shows that the rotation angle is almost constant above the saturation field H_s. Above H_s, the change in the magnetic Faraday rotation is expected to be very small because only the small van Vleck paramagnetism contributes to the increase in the magnetization. The non-magnetic part $\theta_0(H)$ should contribute to the Faraday rotation independently of the saturation of the magnetization and, therefore, we can deduce that $\theta_0(H)$ is negligibly small for NENP. In the case of $CsNiCl_3$, the rotation angle shows saturation between 75 and 100 T. It is thus expected that $\theta_0(H)$ for $CsNiCl_3$ is also very small.

As is discussed in section 3, there are relatively large contributions of the higher-order terms to magnetic Faraday rotation, i.e. the coefficients $A_3, A_5, \ldots$ in equation (1) should be taken into account. For light of lower photon energies than the Γ_2–Γ_5 transition energy,

these higher-order terms would be negligibly small as is discussed in section 2. In the present experiment, we corrected the higher-order terms by comparing the present results of Faraday rotation with the magnetization curve obtained in lower fields obtained by non-destructive magnets. To obtain an analytical formula between the rotation angle θ and the magnetization M, we assume that only the first- and the third-order terms contribute to the Faraday rotation. Let us introduce a normalized magnetization $\tilde{M} = M/M_s$ (M_s is the saturation magnetization) and a normalized magnetic field $\tilde{H} = H/H_s$ and express equation (1) as

$$\theta = A(\tilde{M} + \tilde{A}_3\tilde{M}^3). \tag{2}$$

Comparing the Faraday rotation data with magnetization in non-destructive fields, $\tilde{A}_3 = 0.75$ is determined for NENP from equation (2). Figure 5 shows a plot of the normalized magnetization $\tilde{M}$ derived from the Faraday rotation data by considering the $\tilde{A}_3$ term in equation (2). The dotted line shows the raw Faraday rotation data without the correction. It is normalized to the value at the saturation field. The magnetic field is normalized by the saturation field $H_s = 122$ T.

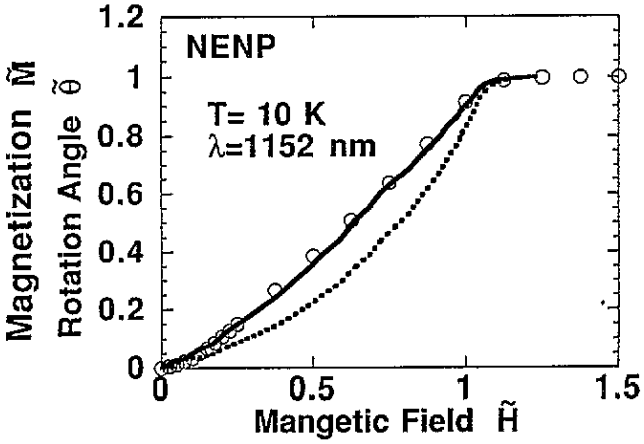

Figure 5. The magnetization curve of NENP: ——, curve obtained by applying the correction of the higher-order contribution to the data in figure 3; ·····, Faraday rotation angle $\tilde{\theta}$ normalized to the value at the saturation; ○, results of Monte Carlo simulation by Yamamoto and Miyashita [19] for $\alpha = 0.2$.

As is shown in section 3, the effect of the finite temperature should be taken into account in the present case. Defining the ratio of the thermal energy to the exchange constant as $\alpha = k_B T/J$ as a measure of the effect of the thermal fluctuation, we have $\alpha \simeq 0.2$ for NENP and $\alpha \simeq 0.35$ for $CsNiCl_3$ in the present experiments. Since α is considerably larger than zero, it is not useful to compare the present data with the magnetization curve calculated at $T = 0$ K. Therefore, we fit the present data with the results of a quantum Monte Carlo simulation of the magnetization curve at a finite temperature by Yamamoto and Miyashita [19]. In figure 5, the result of the Monte Carlo simulation for $\alpha = 0.2$ is plotted together with the present experimental data. They show good agreement with each other. This agreement shows that the magnetization process of the NENP can be quantitatively explained by that of an $S = 1$ one-dimensional Heisenberg antiferromagnet except for the effect by the Haldane gap which was observed around H_c as shown in [15, 16].

A similar procedure is applied for $CsNiCl_3$ and $\tilde{A}_3 = 0.85$ was obtained. The magnetization curve derived from this correction is plotted in figure 6 together with the Faraday rotation data. The magnetic field is normalized by $H_s = 70$ T. The magnetization

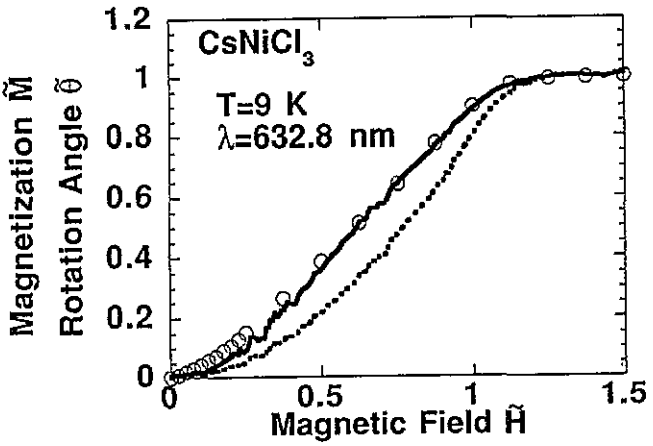

Figure 6. The magnetization curve of $CsNiCl_3$: ——, curve obtained by applying the correction of the higher-order contribution to the data in figure 4: ·····, Faraday rotation angle $\tilde{\theta}$ normalized to the value at the saturation; O, result of Monte Carlo simulation by Yamamoto and Miyashita [19] for $\alpha = 0.3$.

is normalized to the value of 70–110 T saturation. The Monte Carlo simulation data for $\alpha = 0.3$ are also plotted in figure 6. The experimental data again show good agreement with the calculation especially in the high-field range above $\tilde{H} = 0.5$. The small discrepancy below $\tilde{H} = 0.5$ may be caused by the effect of the interchain coupling. The magnetization in higher fields shows that $CsNiCl_3$ also behaves as a one-dimensional Heisenberg antiferromagnet at 9 K. As is mentioned in section 1, $CsNiCl_3$ has a peak in the temperature dependence of the susceptibility at around 35 K, which indicates the development of one-dimensional correlation among spins. In the temperature range between this temperature and the ordering temperature $T_{N1} = 4.84$ K, the system is considered to be in the crossover regime from a one-dimensional to a three-dimensional magnet. The interchain coupling J' is estimated to be as small as $J'/J = (0.2\text{–}5) \times 10^{-2}$ as mentioned in section 1. Therefore, it is reasonable that we observed one-dimensional behaviour of $CsNiCl_3$ in high fields where the interchain coupling J' is smaller than the Zeeman energy.

The saturation field was thus determined as $H_s = 122$ T and $H_s = 70$ T for NENP and $CsNiCl_3$, respectively, by comparison with the Monte Carlo simulation as mentioned above. In the following, we evaluate the exchange coupling constant J from these saturation fields. In the case of one-dimensional Heisenberg antiferromagnets, there is a relation between J and H_s:

$$g\mu_B H_S = 4JS \tag{3}$$

where we define J by the Hamiltonian of the spin system given by

$$H = J \sum_{ij} S_i \cdot S_j. \tag{4}$$

In the case of NENP, from the observed saturation field of $H_s = 122$ T, a value of $J = 45.5$ K is evaluated using the g-value along the a axis, $g_a = 2.23$, which was determined by Meyer *et al* [14]. The present value is in good agreement with the exchange constants of 47.5 K obtained by Meyer *et al* [14] and 55 K by Renard *et al* [13]. The discrepancy of several per cent may be due to the anisotropy which is not included in equation (2).

The exchange constant J is evaluated in a similar way to that for $CsNiCl_3$. The value of $J = 25.8$ K is obtained from $H_s = 70$ T and $g_\perp = 2.2$, the g-value perpendicular to

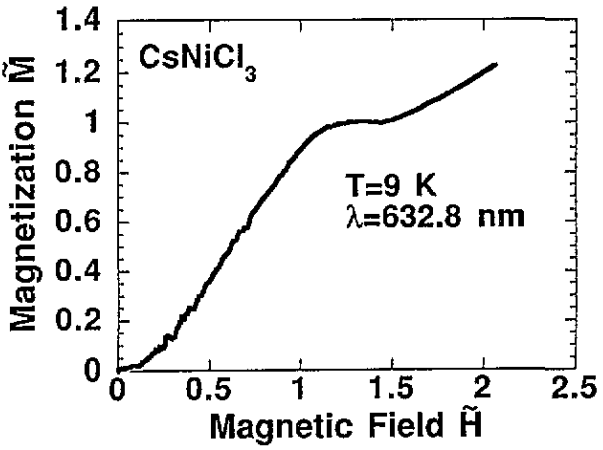

Figure 7. The magnetization curve of $CsNiCl_3$ up to 150 T. The Faraday rotation still shows an increase above 110 T as discussed in section 4.

the c axis by Tanaka *et al* [22]. The present value is in good agreement with the values of 24–33.2 K which are summarized in [11, 12]. The present data for $CsNiCl_3$ are also consistent with the recent result of magnetization measurement obtained by Katori *et al* [23] using an inductive probe.

Finally, we discuss the observed anomalous Faraday rotation above 110 T for $CsNiCl_3$. The magnetization curve up to 150 T obtained by applying the correction of the $\tilde{A}_3$-term in equation (2) is plotted in figure 7. The magnetic field is normalized to 70 T. Above the normalized magnetic field $\tilde{H} = 1.5$, the magnetization shows an almost linear increase against the magnetic field and reaches $\tilde{M} = 1.2$. There are a few possibilities that may cause such an anomalous increase in the Faraday rotation. The first is the crossover between the ground-state orbit and the orbits of the excited state in the ^3F state of Ni^{2+} ions. This is unlikely because the energy splitting between these orbits is considerably larger than the Zeeman energy at 100–150 T. Another possibility is a change in the coefficients A_1 and A_3 in equation (1) associated with the change in the dielectric constant ε caused by the deformation of the lattice. When A_1 and A_3 change, an increase in the Faraday rotation is expected even if the magnetization remains constant. It is interesting whether such a large change in the dielectric constant ε is induced by the high magnetic fields. However, it is not clear at present whether such a change in ε is really possible or whether there is a different mechanism to cause the anomalous Faraday rotation.

5. Summary

Faraday rotation measurements were performed on NENP and $CsNiCl_3$ up to 150 T. In the case of NENP, the saturation of the rotation was observed at around 122 T. There is a large contribution of the higher-order terms to the Faraday rotation at 1152 nm. The correction was performed to evaluate the real magnetization curve assuming that only the first- and the third-order terms contribute to the rotation. The coefficients of these terms were determined by comparing the Faraday rotation data with the magnetization curve in non-destructive pulsed fields. The magnetization curve derived from the Faraday rotation shows good agreement with the result of the Monte Carlo simulation at finite temperatures by Yamamoto and Miyashita. The exchange constant is determined as $J = 45.5$ K from the saturation field and it is consistent with the values reported so far from other experiments. Applying a similar procedure, we derived the magnetization curve for $CsNiCl_3$ and found

good agreement with the result of Monte Carlo simulation. However, there is a small deviation in lower fields which may be caused by the interchain coupling. The exchange constant is evaluated as $J = 25.8$ K which is consistent with the exchange constant so far reported for this material. An anomalous increase in the Faraday rotation was observed above 110 T.

References

[1] Haldane F D M 1983 *Phys. Rev. Lett.* **50** 1153
[2] Buyers W J L, Morra R M, Armstrong R L, Hogan M J, Gerlach P and Hirakawa K 1986 *Phys. Rev. Lett.* **56** 371
[3] Steiner M, Kakurai K, Kjems J K, Petitgrand D and Pynn R 1987 *J. Appl. Phys.* **61** 3953
[4] Achiwa N 1969 *J. Phys. Soc. Japan* **27** 561
[5] Minkiewicz V J, Cox D E and Shirane G 1971 *Solid State Commun.* **8** 1001
[6] Mekata M, Adachi K, Takagi H and Achiwa N 1970 *Proc. 12th Int. Conf. and Low Temperature Physics* ed E Kanda (Tokyo: Keigako) p 801
[7] Cox D E and Minkiewicz V J 1971 *Phys. Rev.* B **4** 2209
[8] Clark R H and Moulton W G 1972 *Phys. Rev.* B **5** 788
[9] Adachi K and Mekata M 1973 *J. Phys. Soc. Japan* **34** 269
[10] Kadowaki H, Ubukoshi H and Hirakawa K 1987 *J. Phys. Soc. Japan* **56** 751
[11] Kakurai K, Steiner M, Pynn R and Kjems J K 1991 *J. Phys.: Condens. Matter* **3** 715
[12] Palme W, Kriegelstein H, Born O, Chennaoui A and Lüthi B 1993 *Z. Phys.* B **92** 1
[13] Renard J P, Verdaguer M, Regnault L P, Erkelens W A C, Rossat-Mignod J and Stirling W G 1987 *Europhys. Lett.* **3** 945
[14] Meyer A, Gleizes A, Girend J J, Verdaguer M and Kahn O 1982 *Inorg. Chem.* **21** 1729
[15] Ajiro Y, Goto T, Kikuchi H, Sakakibara T and Inami T 1989 *Phys. Rev. Lett.* **63** 1424
[16] Katsumata K, Hori H, Takeuchi T, Date M, Yamagishi A and Renard J P 1989 *Phys. Rev. Lett.* **63** 86
[17] Parkinson J B and Bonner J C 1985 *Phys. Rev.* B **32** 4703
[18] Sakai T and Takahashi M 1991 *Phys. Rev.* B **43** 13383
[19] Yamamoto S and Miyashita S 1995 *Phys. Rev.* B **51** 3649
[20] Nakao K, Herlach F, Goto T, Takeyama S, Sakakibara T and Miura N 1985 *J. Phys. E: Sci. Instrum.* **18** 1018
[21] Ackerman J, Holt E M and Holt S L 1974 *J. Solid State. Chem.* **9** 279
[22] Tanaka H, Teraoka S, Kakehashi E, Iio K and Nagata K 1988 *J. Phys. Soc. Japan* **57** 3979
[23] Katori H A, Ajiro Y, Asano T and Goto T 1995 *J. Phys. Soc. Japan* at press